# Effects of Ion Exchange on the Structure of ETS-10

Yuni K. Krisnandi, Eric E. Lachowski, and Russell F. Howe*

*Department of Chemistry, University of Aberdeen, AB24 3UE, Scotland*

*Received August 10, 2005. Revised Manuscript Received November 10, 2005*

A detailed characterization study is reported of ETS-10 subjected to ammonium ion exchange and subsequent sodium ion back exchange. It is shown that although such ion exchange leaves the crystallinity of ETS-10 measured by X-ray powder diffraction unchanged, other techniques reveal that the structure becomes locally damaged. In particular, there is partial dissolution of silica from the outer regions of ETS-10 crystallites under low pH conditions, exposing titania-rich surface sites and substantially modifying the photoreactivity of the material.

## Introduction

ETS-10 is the most widely recognized member of the titanosilicate microporous group. The structure, first established in 1995 from a combination of HRTEM, NMR, and molecular modeling techniques[1] and subsequently confirmed from a single-crystal diffraction study,[2] is illustrated schematically in Figure 1. Linear chains of corner-linked $TiO_6$ octahedra run along the *a* and *b* axes, surrounded by tetrahedral silicate units, forming a large-pore three-dimensional channel system. Each $TiO_6$ unit contributes two negative charges to the framework, which are balanced by exchangeable cations.

The high cation exchange capacity of ETS-10 has attracted some attention.[3−6] In comparison with conventional aluminosilicate zeolites, however, the intrinsically disordered nature of the ETS-10 structure may impose some limitations on practical applications. The actual crystal structure comprises intergrowths of polymorphs containing different stacking sequences of titanosilicate layers. (The structure represented in Figure 1 is that of the monoclinic polymorph B.) Stacking faults along the *c* axis produce interrupted titania chains and multiple pores (also represented in Figure 1). We have reported elsewhere spectroscopic studies of a series of differently synthesized ETS-10 crystals that showed that a set of materials having identical X-ray powder diffraction patterns could contain widely varying levels of disorder.[7]

ETS-10 as synthesized usually contains $Na^+$ and $K^+$ as exchangeable cations. Conversion to the proton-exchanged form may be done by direct acid exchange at low pH, or via $NH_4^+$ exchange followed by thermal evolution of $NH_3$. We have found that the photocatalytic reactivity of ETS-10 is strongly influenced by whether the material is as-synthesized or proton-exchanged.[8,9] Mild acid treatment has also been reported by others to significantly modify the photocatalytic activity and selectivity of ETS-10.[10,11] This has prompted us to investigate spectroscopically the effects of typical ion-exchange procedures on both local and long-range structure of ETS-10, in the hope of better understanding variability of the photoreactivity. This paper reports that the ETS-10 structure is much more fragile than had previously been recognized and that ion exchange at low pH causes extensive damage to the external surfaces of ETS-10 crystals, dissolving silica and leaving exposed titania sites with photoreactivity similar to that of anatase.

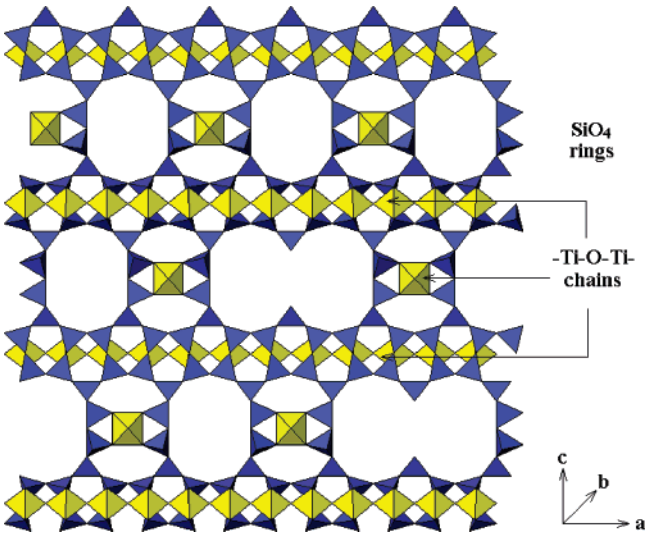


**Figure 1.** Structure of ETS-10. The yellow polyhedra are $TiO_6$ octahedra running in the *a* and *b* directions. The blue polyhedra are $SiO_4$ tetrahedra forming 12-ring pores. Double pores arise from stacking faults in the inherently disordered material.

* Corresponding author. E-mail: r.howe@abdn.ac.uk.

(1) Anderson, M. W.; Terasaki, O.; Ohsuna, T.; Omalley, P. J.; Philippou, A.; Mackay, S. P.; Ferreire, A.; Rocha, J.; Lidin, S. *Philos. Magn. B* **1995**, *71*, 813−841.
(2) Wang, X.; Jacobson, A. J. *Chem. Commun*. **1999**, 973−974.
(3) Al-Attar, L.; Dyer, A.; Harjula, R. *J. Mater. Chem*. **2003**, *13*, 2963−2974.
(4) Zhao, G. S.; Lee, J. L.; Chia, P. A. *Langmuir* **2003**, *19*, 1977−1979.
(5) Kucznicki, S. M.; Thrush, K. A. U.S. Patent, 4,994,191, 1991.
(6) Gervasini, A.; Picciau, C.; Auroux, A. *Microporous Mesoporous Mater*. **2000**, *35−36*, 457−469.
(7) Southon, P. D.; Howe, R. F. *Chem. Mater*. **2002**, *14*, 4209−4218.
(8) Krisnandi, Y. K.; Southon, P. D.; Adesina, A. A.; Howe, R. F. *Int. J. Photoenergy* **2003**, *5*, 131−140.
(9) Howe, R. F.; Krisnandi, Y. K. *Chem. Commun*. **2001**, 1588−1589.
(10) Calza, P.; Paze, C.; Pelizzetti, E.; Zecchina, A. *Chem. Commun*. **2001**, 2130−2132.
(11) Xamena, F. X.; Calza, P.; Lamberti, C.; Prestiponi, C.; Damin, A.; Bordiga, S.; Pelizzetti, E.; Zecchina, A. *J. Am. Chem. Soc*. **2003**, *125*, 2264−2271.

10.1021/cm051785g CCC: $33.50 
Published on Web 01/20/2006

## Experimental Section

ETS-10 was synthesized hydrothermally from a gel with starting composition 3.7:0.95:1:5.7:171 $Na_2O$:$K_2O$:$TiO_2$:$SiO_2$:$H_2O$. A solution of 1.3 g of NaOH pellets in 9.3 g of distilled water was added to a stirred solution of 10 g of sodium silicate (25.5−28.5 wt % $SiO_2$, 7.5−8.5 wt % $Na_2O$) by dropwise addition of 8.6 g of $TiCl_3$ solution (15 wt % in HCI) with vigorous stirring. Then 1.5 g of dehydrated KF was added, followed by 20 mg of ETS-10 (Engelhard Corporation) as crystallization seeds. The mixture was secured in a 100 mL Teflon-lined autoclave and heated at 473 K for 48 h. The resulting product was filtered, washed, and dried in a desiccator.

$NH_4$ETS-10 was prepared from the as-synthesized (Na,K)ETS-10 by multiple ion exchanges with 1 M $NH_4NO_3$ solutions at 358 K for 36 h (1 g of zeolite in 500 mL of solution). The pH of the solution rose from 4.5 to 6.4 during the ion exchange. Na back-exchanged samples were prepared by treating $NH_4$ETS-10 samples with 1 M $NaNO_3$ solution under similar conditions. In this case the pH fell from 5.2 to 3.5 during the ion exchange. After ion exchange, samples were filtered, washed, and air-dried at 373 K.

X-ray powder diffraction patterns were obtained with a Bruker Avance D8 diffractometer using Cu Kα radiation. Scanning and transmission electron microscopy, electron diffraction, and EDX analysis were undertaken on a JEOL 2000 TEMSCAN instrument (using aluminum evaporated onto the carbon support as an internal standard for electron diffraction measurements). Raman spectra were recorded with a Renishaw Raman 2000 microprobe, using 785 nm excitation. $^{29}$Si NMR spectra were recorded with a Varian Infinity Plus 400 MHz spectrometer using 90° pulses of 5 $\mu$s, a 60 s pulse delay, and spinning rate of 3 kHz. All $^{29}$Si chemical shifts were referenced to TMS via a kaolin secondary standard. Infrared spectra were collected from pressed disks of sample mounted in a high-vacuum cell allowing in situ outgassing, using a Nicolet Magna instrument at 4 $cm^{-1}$ resolution.

X-ray photoelectron spectra were obtained from pressed disks of sample using a VG Escalab II instrument (Al Kα radiation, 1486.6 eV). X-ray absorption spectra were recorded at BM29, ESRF, Grenoble. Pressed disks of sample were measured in transmission mode using a 10 K cryostat at the titanium K-edge. Ti foil was used to calibrate the monochromator and the near-edge spectrum was recorded at a resolution of 0.2 eV.

## Results and Discussion

The as-synthesized (Na,K)ETS-10 sample used as the starting material in this work gave a powder diffraction pattern identical to those reported previously for ETS-10 (Figure 2a). The $^{29}$Si NMR spectrum of the starting material (Figure 3a) likewise is closely similar to that reported for well-crystalline ETS-10, showing a group of four peaks between −94 and −97 ppm due to silicon bonded through oxygen to three silicons and a titanium and a fifth peak at −103.4 ppm due to silicon bonded through oxygen to four silicons.[1] This characteristic $^{29}$Si NMR signature together with an intense narrow Raman band at 724 $cm^{-1}$ (Figure 4a) due to the totally symmetric combination of coupled Ti−O stretching modes in the octahedral titania chains[12] indicates that the (Na,K)ETS-10 sample is relatively free of stacking faults and resembles the most highly ordered of the suite of samples described previously.[7]

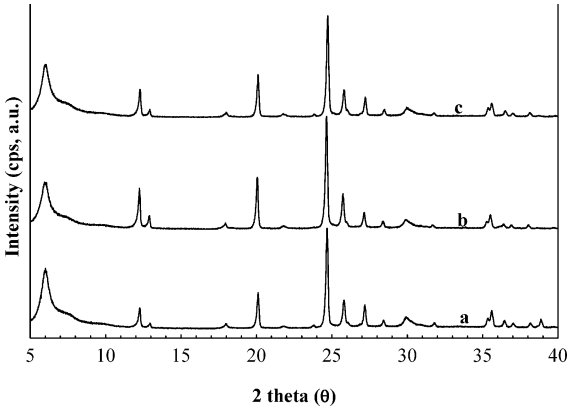


**Figure 2.** X-ray powder diffraction patterns of (a) (Na, K) ETS-10 as-synthesized, (b) $NH_4^+$-exchanged, and (c) $Na^+$ back-exchanged samples.

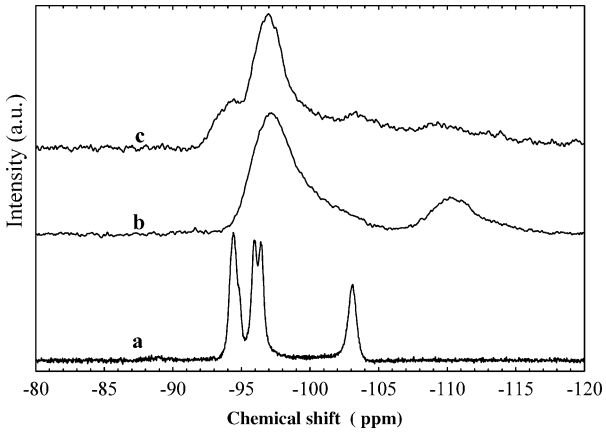


**Figure 3.** $^{29}$Si NMR spectra of (a) (Na, K) ETS-10 as-synthesized, (b) $NH_4^+$-exchanged, and (c) $Na^+$ back-exchanged samples.

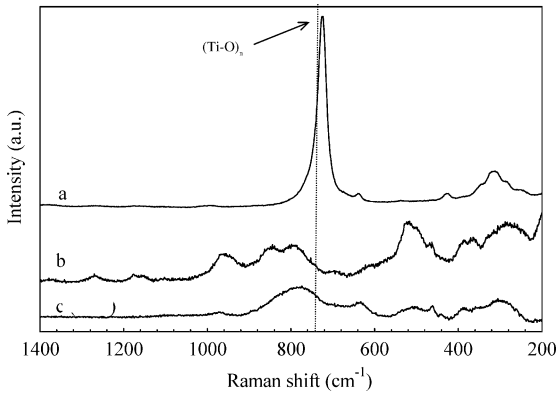


**Figure 4.** Raman spectra of (a) (Na, K) ETS-10, (b) $NH_4^+$-exchanged, and (c) $Na^+$ back-exchanged samples.

Ammonium ion exchange, and subsequent sodium ion back exchange, cause no discernible changes to the X-ray powder diffraction pattern of ETS-10 (Figure 2). Ion exchange does however dramatically alter the $^{29}$Si NMR spectra (Figure 3). After ammonium exchange, the $Q_3$ silicon signals broaden and merge into a single broad band shifted upfield, while the $Q_4$ silicon peak is broadened and shifted even further, to about −110 ppm. Similar $^{29}$Si NMR spectra have been reported previously by Yang and Blosser[13] for

(12) Damin, A.; Xamena, F. X.; Lamberti, C.; Civalleri, B.; Zicovich-Wilson, C. M.; Zecchina, A. *J. Phys. Chem. B* **2004**, *108*, 1328−1336.

(13) Yang, X.; Blosser, P. W. *Zeolites* **1996**, *17*, 237−243.

proton-exchanged ETS-10. These authors attributed changes in the spectra on proton exchange to alteration of the local charge density at silicon sites, or to structural changes in bond angles, although they also suggest that silanol hydroxyl group defect formation may be occurring. Cation exchange in zeolites is known to alter $^{29}$Si chemical shifts by up to 5 ppm.[14]

Infrared spectra of ammonium-exchanged samples (not shown) confirmed that ammonium exchange had occurred. On back exchange, the ammonium ion stretching and bending modes reduced to ca. 20% of their original intensity, indicating about 80% replacement of $NH_4^+$ by $Na^+$. XPS analysis also confirmed the replacement of $Na^+$ and $K^+$ by $NH_4^+$ on ammonium ion exchange, and replacement of $NH_4^+$ by $Na^+$ on back exchange, in the outer regions of the ETS-10 crystals.

The $^{29}$Si NMR spectrum of the starting material was not restored on back exchange (Figure 3c). The back-exchanged sample shows component signals with chemical shifts comparable to those of the starting material, but with dramatically increased line widths. This indicates that the chemical shift changes occurring on ion exchange may be related to the cations present (and hence the local charge density, as suggested in refs 13 and 14). However, the increase in line width is irreversible.

Further spectroscopic evidence for the irreversibility of the ammonium exchange back-exchange process comes from the Raman spectra shown in Figure 4. The intense 724 $cm^{-1}$ band due to coupled Ti−O stretching modes was completely removed on ammonium ion exchange and back exchange with $Na^+$ left a broad weak bank at about 790 $cm^{-1}$. This spectrum (Figure 4c) is closely similar to that of the most disordered form of ETS-10 in the series of samples described previously,[7] suggesting strongly that ion exchange has introduced significant disorder into the structure. Xamena et al. have also reported broadening and shifting to higher frequency of the 724 $cm^{-1}$ band when ETS-10 was subjected to a mild etching with HF.[15]

The suggestion of structural modification is confirmed by electron microscopy examination of ion-exchanged samples. Figure 5 shows SEM images of the as-synthesized starting material, ammonium-exchanged and back-exchanged samples. Crystals of the starting material show a well-defined morphology, mainly cuboid, with some evidence of layering due to polymorph intergrowth. The crystal surfaces become substantially roughened after ammonium ion exchange, although they retain the original morphology. After sodium back exchange, the crystal surfaces become even more dramatically damaged, with fragmentation into smaller particles about 100 nm in size.

Further evidence of crystal damage as a result of ion exchange is seen in low-resolution TEM images in Figure 6. Ammonium exchange clearly damages the outer edges of the crystals (Figure 6b, while more extensive cracking and internal damage is seen in the back-exchanged samples (Figure 6c).

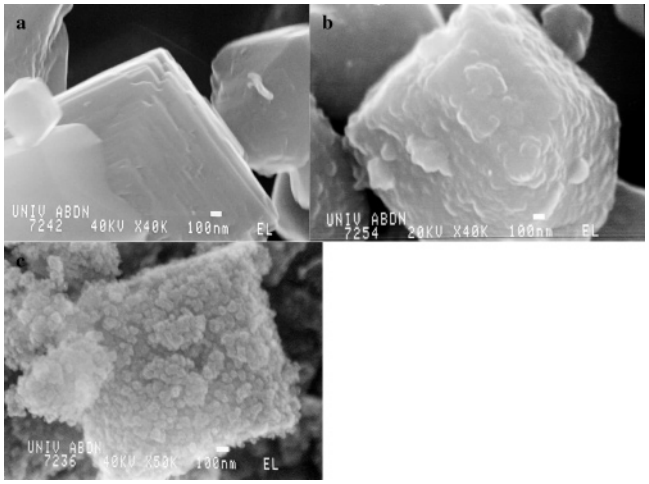


**Figure 5.** Scanning electron microscope images of (a) (Na, K) ETS-10, (b) $NH_4^+$-exchanged, and (c) $Na^+$ back-exchanged samples. Scale bar is 0.1 $\mu$m in each case, and crystals are about 2 $\mu$m in size.

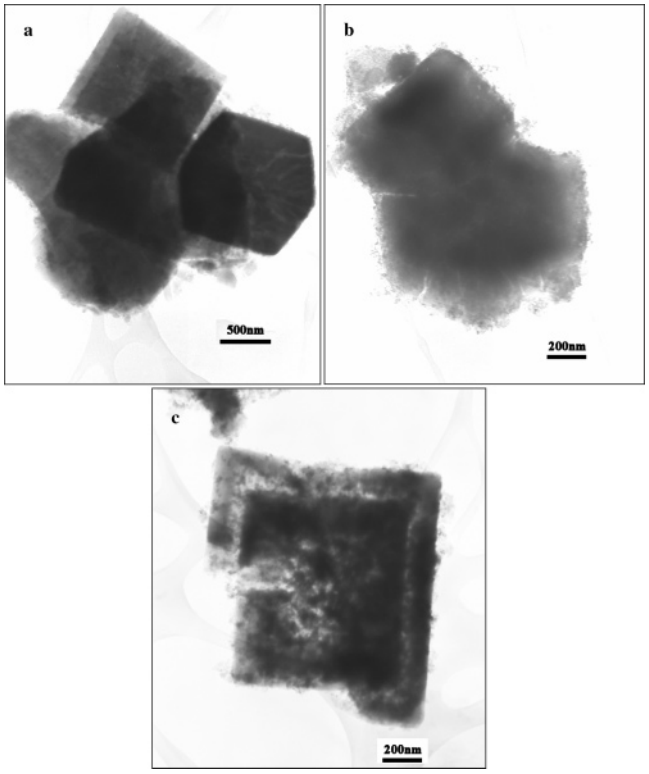


**Figure 6.** Transmission electron micrographs of (a) (Na, K) ETS-10, (b) $NH_4^+$-exchanged, and (c) $Na^+$ back-exchanged samples.

**Table 1. EDX and XPS Analyses**[a]

| sample | Ti:Si (bulk) | Ti:Si (Edge) | Ti:Si (XPS) |
|---|---|---|---|
| as-synthesized | 0.23 ± 0.01 | | 0.12 |
| $NH_4^+$-exchanged | 0.25 ± 0.02 | 0.22 ± 0.04 | 0.24 |
| $Na^+$-exchanged | 0.43 ± 0.06 | 0.57 ± 0.20 | 0.33 |

[a] Error bars on EDX analyses reflect variations in analyses from different sample points. Bulk composition Ti:Si = 0.20.

Table 1 gives the results of EDX analyses of elemental ratios in different regions of the crystals and compares these with XPS analyses of the surface Ti:Si ratios. The starting material gives an EDX analysis comparable with the theoretical bulk composition of ETS-10. The XPS analysis

(14) Engelhardt, G.; Michel, D. *High-Resolution Solid State NMR of Silicates and Zeolites*; Wiley: New York, 1987.
(15) Xamena, F. X.; Damin, A.; Bordiga, S.; Zecchina, A. *Chem. Commun.* **2003**, 1514−1515.

**Table 2. ICP-MS Analyses of Solutions Contacted with (Na, K) ETS-10[a]**

| solution | initial pH | final pH | solution concentration (ppb) Si | solution concentration (ppb) Ti | framework atoms dissolved (%) Si | framework atoms dissolved (%) Ti |
|---|---|---|---|---|---|---|
| distilled water | 7.0 | 10.0 | 131 | 7.4 | 2.1 ± 0.2 | 0.35 ± 0.05 |
| 1 M $NH_4NO_3$ | 4.5 | 6.4 | 446 | 2.3 | 7.2 ± 0.4 | 0.1 ± 0.05 |
| 1 M $NaNO_3$ | 5.2 | 8.1 | 124 | 2.0 | 2.0 ± 0.4 | 0.1 ± 0.05 |

[a] 12 h exposure for $NH_4NO_3$ and $NaNO_3$, 24 h for distilled water.

shows a silicon-rich outer surface, as expected for analysis by this surface-sensitive technique. After ammonium ion exchange, the surface Ti:Si ratio measured by XPS increases, although EDX detects little difference between the interior and the edges of the crystals. After $Na^+$ back exchange, it is clear however that Ti:Si ratios have increased both at the surface and in the interior of crystals. The wider variability in the EDX results for back-exchanged samples also indicates the greater heterogeneity of these samples.

These analyses of ion-exchanged crystals suggest selective loss of silicon under ion-exchange conditions. This was confirmed by undertaking ICP-MS analyses of solutions contacted with ETS-10 under conditions similar to those of ion exchange. Analytical results from these solutions are listed in Table 2. Some dissolution of silica and titania occurs in distilled water when the pH was measured to rise to 10 after 24 h exposure. Silica dissolution is most pronounced however under the lower pH conditions of ammonium ion exchange, when as much as 7% of the silicon initially present in ETS-10 is found as soluble species. The dissolution of titanium under these conditions is barely measurable.

The loss of silica from the outer regions of the ETS-10 crystals during ion exchange raises the question of what form the remaining titania is in. Selected area electron diffraction measurements provide information about structure changes. Figure 7 shows a set of electron diffraction patterns taken from the as-synthesised ETS-10, after ammonium ion exchange and after sodium back exchange. Figure 7a is an [001] zone axis pattern of a tetragonal crystal (polymorph A) in the as-synthesized ETS-10. Figure 7b shows the [010] zone axis pattern of a tetragonal crystal from an ammonium-exchanged sample. It shows the characteristic streaking parallel to $c^*$ when $h$ is odd. Figure 7c shows the [001] zone axis pattern of a crystal after sodium back exchange; in this case the crystal is monoclinic (polymorph B), reflecting the presence of both polymorphs in ETS-10. The patterns in Figures 7b and 7c were taken from the center of the crystals. On the other hand, the patterns in Figures 7d and 7e were taken from the edges of ammonium- and sodium back-exchanged crystals, respectively. They show that the edges are polycrystalline, giving a ring pattern with some diffuse scattering from an amorphous component The faintness of these additional rings precludes accurate $d$ spacing measurements, but the approximate values of 3.54 and 1.82 Å correspond well with those expected for anatase (3.52 Å, $I = 100$, and 1.89 Å, $I = 35$). The strong spots still appearing in Figures 7d and 7e are due to reflections from the undamaged interior of crystals which cannot be totally excluded from the regions analyzed. The electron diffraction data suggest therefore that the outer regions of the ion-exchanged crystals which have been depleted in silica contain either anatase or at least a poorly crystalline anatase precursor.

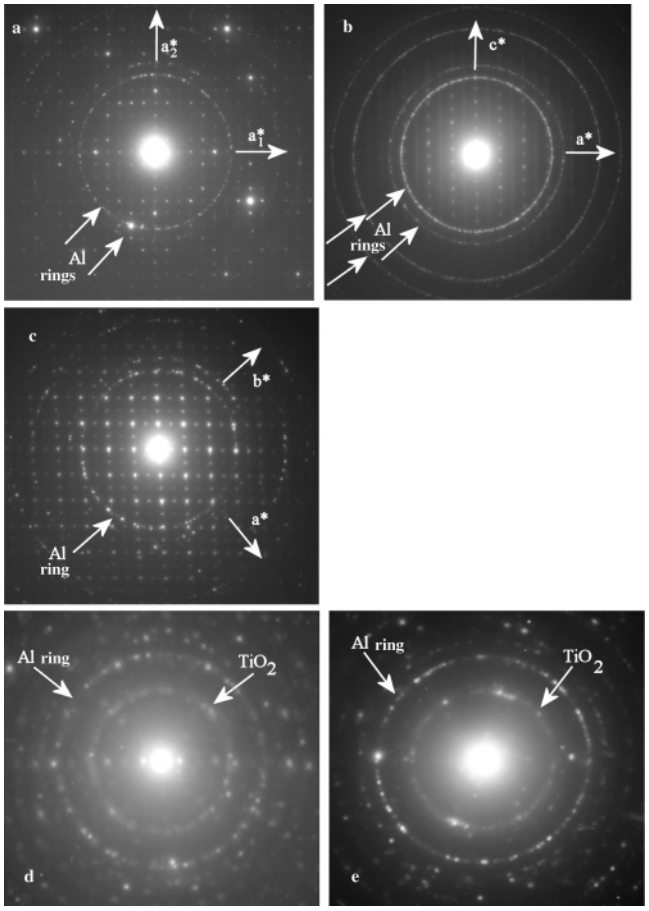


**Figure 7.** Selected area electron diffraction patterns from (a) (Na, K) ETS-10, (b) center of an $NH_4^+$-exchanged crystal, (c) center of an $Na^+$ back-exchanged crystal, (d) edge of an $NH_4^+$-exchanged crystal, and (e) edge of a $Na^+$ back-exchanged crystal.

Further support for this conclusion comes from the titanium K-edge XANES data shown in Figure 8. The as-synthesized (Na, K) ETS-10 shows a prominent pre-edge peak at around 4971 eV associated with the distorted octahedral coordination of $Ti^{4+}$ in the titania chains.[16] (The pre-edge peak is due to 1s → 3d transitions which are forbidden in strict octahedral symmetry.) This peak broadens on ion exchange, and two additional pre-edge components at 4968.7 and 4974.2 eV, which are barely visible in the starting material, become more prominent. After $Na^+$ back exchange, the pre-edge spectrum contains similar features, albeit with different relative intensities, to those found in the spectrum of anatase (Figure 8e). The XANES data thus imply that the titanium environment in the ion-exchanged samples more closely resembles that in anatase than in the as-synthesized ETS-10.

Ti K-edge EXAFS data were also collected from the same set of samples. Figure 9 shows the normalized Fourier transforms of the EXAFS. The EXAFS and Fourier transforms of the as-synthesized material can be fitted to a structural model consistent with the known structure of ETS-

(16) Prestipinio, C.; Solari, P. L.; Lamberti, C. *J. Phys. Chem. B* **2005**, *109*, 13132−13137.

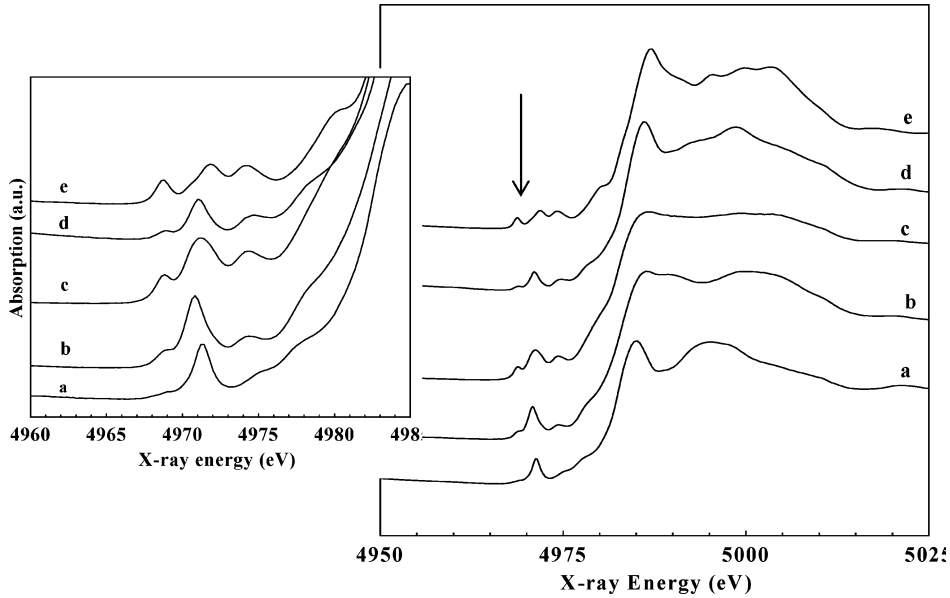


**Figure 8.** Ti K-edge XANES data for (a) (Na, K) ETS-10, (b) $NH_4^+$-exchanged sample, (c) and (d) two different $Na^+$ back-exchanged samples, and (e) anatase. Inset shows expansion of region around 4970 eV.

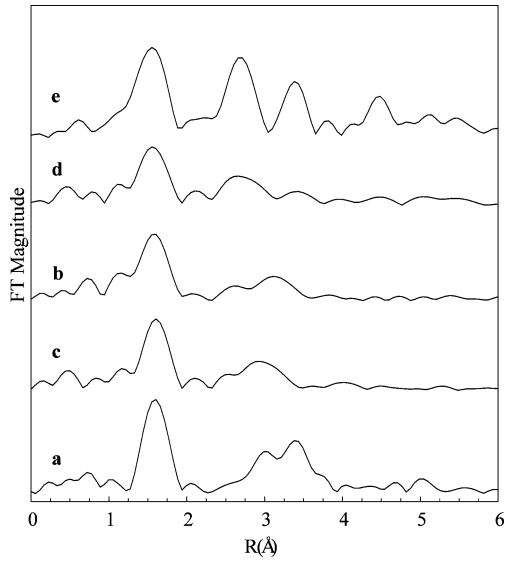


**Figure 9.** Ti K-edge EXAFS data for (a) (Na, K) ETS-10, (b) $NH_4^+$-exchanged sample, (c) and (d) two different $Na^+$ back-exchanged samples, and (e) anatase.

10. There is some controversy in the literature concerning the extent to which the Ti K-edge EXAFS of ETS-10 is either consistent with[16] or contradicts[17] the single-crystal X-ray structure which shows equal Ti−O distances along the titania chains.[2] Our own data for a number of different as-synthesized ETS-10 samples are best fitted to the structural model proposed by Sankar et al.,[17] which does not agree with the single-crystal structure. We will discuss this aspect of the structure of ETS-10 in more detail elsewhere.[18] The important point in the present work is that for the ion-exchanged samples the second shell contributions to the EXAFS become dramatically reduced, indicating loss of long-range order in the Ti−O−Ti−O chains. In back-exchanged samples it is even possible to recognize components of the anatase Fourier transform also shown in Figure 9. The obvious heterogeneity of the samples precludes however any attempt at fitting the data to a structural model.

An important issue for the photoreactivity of ETS-10 is the extent to which the structural modifications caused by ion-exchange treatments modify the UV−visible absorption spectrum of ETS-10. Figure 10 compares the reflectance spectrum of the starting material with those of the ion-exchanged samples and with anatase. The apparent band gap of each sample was taken as the point of maximum slope on the absorption edge, as determined by the derivative traces in the figure inset.

It is clear that ion exchange causes a significant red shift in the apparent band gap of ETS-10 by about 0.2 eV. The absorption edge shifts closer to that of anatase. At the same time there is an increased tailing of the absorption edge into the visible region of the spectrum, very reminiscent of that seen in nanoparticulate anatase containing high concentrations of defects, which introduce levels into the band gap.[19]

The photoreactivity of the ion-exchanged ETS-10 samples is described in detail elsewhere.[20] In summary, the key differences between the as-synthesized and ion-exchanged samples are as follows:

UV irradiation in the presence of ethene (a hole scavenger) causes photoreduction of Ti(IV) to Ti(III) in the ion-exchanged samples, but not in the as-synthesized material. This is attributed to trapping of electrons at exposed Ti(IV) sites in the damaged samples.

UV irradiation in the presence of oxygen forms the superoxide ion $O_2^-$ in ion-exchanged samples, but not in the as-synthesized material. The superoxide ion is adsorbed at exposed $Ti^{4+}$ sites and is formed through trapping of photogenerated electrons by oxygen.

UV irradiation in the presence of oxygen and ethene together causes some partial oxidation to adsorbed carbonyl

(17) Sankar, G.; Bell, R. C.; Thomas, J. M.; Anderson, M. W.; Wright, P. A.; Rocha, J. *J. Phys. Chem.* **1996**, *100*, 449−452.
(18) Southon, P. D.; Krisnandi, Y. K.; Howe, R. F. To be published.
(19) Luca, V.; Djajanti, S.; Howe, R. F. *J. Phys. Chem. B* **1998**, *102*, 10650−10657.
(20) Krisnandi, Y.; Howe, R. F. *Appl. Catal. A*, in press.

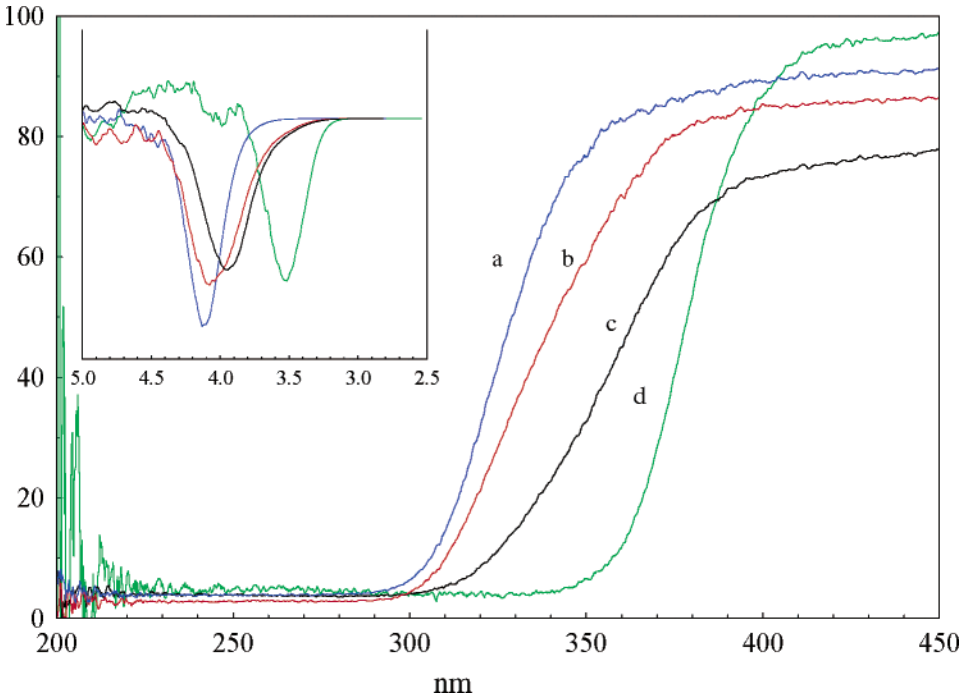


**Figure 10.** Diffuse reflectance UV−Vis spectra of (a) (Na, K) ETS-10, (b) $NH_4^+$-exchanged sample, (c) $Na^+$ back-exchanged sample, and (d) anatase. Inset shows first derivatives in the vicinity of the absorption edge, in eV units.

compounds (acetaldehyde, acetic acid) in all three samples, but this occurs to a much greater extent in the ion-exchanged samples.

We conclude that the ion-exchanged samples behave, in terms of photoreactivity, quite similarly to anatase. This similarity can now be understood from the data presented here that show that the ion-exchange treatments, under mildly acidic pH conditions, expose titanium sites on the external surface or in fissures within crystals through partial dissolution of silica. The fragility of ETS-10 toward ion-exchange treatment has not been previously appreciated. From the viewpoint of photocatalysis, our results agree with the findings of others[11] that damaged ETS-10 may be a better photocatalyst than well-crystalline examples.

**Acknowledgment.** This work has been supported in part by the University of Aberdeen and in part by the donors of the Petroleum Research Fund of the American Chemical Society. Y.K. acknowledges also the award of a UK Overseas Research Studentship. We thank also Dr. Andrea Raab for assistance with the ICP-MS measurements.

CM051785G